Hyperbolic geometry for colour metrics

Ivar Farup[*]

Faculty of Computer Science and Media Technology, Gjøvik University College, Norway

[*]*ivar.farup@hig.no*

Abstract: It is well established from both colour difference and colour order perpectives that the colour space cannot be Euclidean. In spite of this, most colour spaces still in use today are Euclidean, and the best Euclidean colour metrics are performing comparably to state-of-the-art non-Euclidean metrics. In this paper, it is shown that a transformation from Euclidean to hyperbolic geometry (i.e., constant negative curvature) for the chromatic plane can significantly improve the performance of Euclidean colour metrics to the point where they are statistically significantly better than state-of-the-art non-Euclidean metrics on standard data sets. The resulting hyperbolic geometry nicely models both qualitatively and quantitatively the hue super-importance phenomenon observed in colour order systems.

© 2014 Optical Society of America

References and links

1. S. M. Newhall, D. Nickerson, and D. B. Judd, "Final report of the OSA subcommittee on the spacing of the Munsell colors," J. Opt. Soc. Am. **33**, 385–411 (1943).
2. D. B. Judd, "Ideal color space – II. The super-importance of hue differences and its bearing on the geometry of color space," Palette **30**, 21–28 (1969).
3. R. G. Kuehni and A. Schwarz, *Color Ordered* (Oxford University Press, 2008).
4. L. Silberstein, "Investigations on the intrinsic properties of the color domain. II," J. Opt. Soc. Am. **33**, 1–9 (1943).
5. D. L. MacAdam, "Visual sensitivities to color differences in daylight," J. Opt. Soc. Am. **32**, 247–274 (1942).
6. D. L. MacAdam, "On the geometry of color space," J. Franklin I. **238**, 195–210 (1944).
7. F. Clarke, R. McDonald, and B. Rigg, "Modification to the JPC79 colour–difference formula," J. Soc. Dyers Colour. **100**, 128–132 (1984).
8. R. McDonald and K. J. Smith, "CIE94 – A new colour-difference formula," J. Soc. Dyers Colour. **111**, 376–379 (1995).
9. M. R. Luo, G. Cui, and B. Rigg, "The development of the CIE 2000 colour-difference formula: CIEDE2000," Color Res. Appl. **26**, 340–350 (2001).
10. D. R. Pant and I. Farup, "Riemannian formulation and comparison of color difference formulas," Color Res. Appl. **37**, 429–440 (2012).
11. M. Nölle, M. Suda, W. Boxleitner, and I. Glendinning, "H2SI – a new perceptual colour space," in "18th International Conference on Digital Signal Processing (DSP)," (IEEE, 2013), pp. 1–6.
12. B. Riemann, "Ueber die Hypothesen, welche der Geometrie zu Grunde liegen, Abh," Ge. Wiss. Gött **13**, 133–152 (1868).
13. H. v. Helmholtz, "Versuch einer erweiterten Anwendung des Fechnerschen Gesetzes im farbensystem," Z. Psychol. Physiol. Sinnesorg. **2**, 1–30 (1891).
14. E. Schrödinger, "Grundlinien einer Theorie der Farbenmetrik im Tagessehen (III. Mitteilung)," Ann. Phys. **368**, 481–520 (1920).
15. W. S. Stiles, "A modified Helmholtz line-element in brightness-colour space," P. Phys. Soc. **58**, 41–65 (1946).
16. A. Ashtekar, A. Corichi, and M. Pierri, "Geometry in color perception," in "Black Holes, Gravitational Radiation and the Universe," (Springer, 1999), pp. 535–550.
17. J. Chao, I. Osugi, and M. Suzuki, "On definitions and construction of uniform color space," in "CGIV 2004: The Second European Conference on Colour in Graphics, Imaging and Vision," (2004), pp. 55–60.

18. J. Chao, R. Lenz, D. Matsumoto, and T. Nakamura, "Riemann geometry for color characterization and mapping," in "Conference on Colour in Graphics, Imaging, and Vision," (Society for Imaging Science and Technology, 2008), pp. 277–282.

19. S. Ohshima, R. Mochizuki, J. Chao, and R. Lenz, "Color reproduction using riemann normal coordinates," in "Computational Color Imaging," (Springer, 2009), pp. 140–149.

20. D. R. Pant and I. Farup, "Geodesic calculation of color difference formulas and comparison with the Munsell color order system," Color Res. Appl. **38**, 259–266 (2013).

21. H. L. Resnikoff, "Differential geometry and color perception," J. Math. Biol. **1**, 97–131 (1974).

22. R. Lenz, T. H. Bui, and J. Hernández-Andrés, "Group theoretical structure of spectral spaces," J. Math. Imaging Vis. **23**, 297–313 (2005).

23. R. Lenz, P. Latorre Carmona, and P. Meer, "The hyperbolic geometry of illumination-induced chromaticity changes," in "Computer Vision and Pattern Recognition, 2007. CVPR'07. IEEE Conference on," (IEEE, 2007), pp. 1–6.

24. J. W. Anderson, *Hyperbolic geometry* (Springer, 2005), 2nd ed.

25. G. Cui, M. Luo, B. Rigg, G. Roesler, and K. Witt, "Uniform colour spaces based on the DIN99 colour-difference formula," Color Res. Appl. **27**, 282–290 (2002).

26. C. Oleari, M. Melgosa, and R. Huertas, "Euclidean color-difference formula for small–medium color differences in log-compressed OSA-UCS space," J. Opt. Soc. Am. A **26**, 121–134 (2009).

27. R. S. Berns, D. H. Alman, L. Reniff, G. D. Snyder, and M. R. Balonon-Rosen, "Visual determination of suprathreshold color-difference tolerances using probit analysis," Color Res. Appl. **16**, 297–316 (1991).

28. R. S. Berns and B. Hou, "RIT-DuPont supra-threshold color-tolerance individual color-difference pair dataset," Color Res. Appl. **35**, 274–283 (2010).

29. P. A. García, R. Huertas, M. Melgosa, and G. Cui, "Measurement of the relationship between perceived and computed color differences," J. Opt. Soc. Am. A **24**, 1823–1829 (2007).

30. D. R. Pant, I. Farup, and M. Melgosa, "Analysis of three Euclidean color-difference formulas for predicting the average RIT-DuPont color-difference ellipsoids," in "Proceedings of AIC2013 – 12th International AIC Congress," (2013), pp. 537–540.

31. M. Luo and B. Rigg, "Chromaticity-discrimination ellipses for surface colours," Color Res. Appl. **11**, 25–42 (1986).

32. G. Wyszecki and G. H. Fielder, "New color-matching ellipses," J. Opt. Soc. Am. **61**, 1135–1152 (1971).

33. M. Melgosa, E. Hita, A. Poza, D. H. Alman, and R. S. Berns, "Suprathreshold color-difference ellipsoids for surface colors," Color Res. Appl. **22**, 148–155 (1997).

1. Introduction

It was early discovered that it is not possible to construct a colour space that scales the Munsell hue and chroma scales such that the resulting chromatic diagram appears uniform [1]. In particular, it was found that the total hue angle of a hypothetic uniform chromatic diagram would have to be significantly greater than 2π. A similar challenge was found during the construction of the perceptually uniform OSA colour space. Judd [2] named the phenomenon 'hue super-importance'. Due to the hue super-importance – which in the first place was observed from a colour order point of view – a perceptually isotropic colour solid cannot be represented in Euclidean space. Circles with total angles greater than 2π are only found in negatively curved spaces. A thorough overview of this issue is given by Kuehni [3].

From a colour metric point of view, it was established already by Silberstein [4] that MacAdam's ellipses [5] for colour discrimination thresholds describes a plane of varying, mainly negative curvature. MacAdam made a physical model for this negatively curved chromatic surface [6]. For supra-threshold experiments, metrics that implicitly define negatively curved chromatic planes, such as CMC($\ell : c$) [7], CIE94 [8], and CIEDE2000 [9], give good fit to the experimentally observed colour differences.

The above observations all suggest that the perceptual colour space has negative curvature. Judd [2] suggested that the chromatic plane can be modelled as a folded fan in order to achieve hue cirles of a total angle greater than 2π. However, such a model would have zero curvature everywhere, except at the centre, where the curvature would be undefined. Similar problems exist for the colour space underlying CIEDE2000, as pointed out recently [10], and also for the newly developed perceptual colour space with hue super-importance, H2SI, by Nölle et al. [11].

Models and analyses of curved colour spaces represented as non-Euclidean spaces have been developed from first-principles in the past. Already Riemann used colour as an illustration of the applicability of his geometry [12], and concrete examples of such colour geometries were developed by Helmholz [13], Schrödinger [14], Stiles [15], Ashtekar et al. [16], and others. Chao et al. [17–19] used geodesic grids for colour transformaions, and Pant and Farup analysed colour metrics in Riemannian space [20]. Although Riemannian geometry gives plenty of flexibility for designing the local properties of the colour space in detail, it is challenging, at best, to exploit this freedom constructively.

The simplest possible space with negative curvature is the hyperbolic space. It has a constant negative curvature everywhere, and thus has circles with angular subtense greater than 2π. In 1974, Resnikoff [21] reasoned from an axiomatic point of view that colour space must be isomorphic to either $\mathbb{R}^+ \times \mathbb{R}^+ \times \mathbb{R}^+$, or $\mathbb{R}^+ \times SL(2,\mathbb{R})/SO(2)$, or, in other words, have either Euclidean or hyperbolic geometry. Even though not all of his axioms might hold true today, the derivation is still enlightening, and the result interesting. Lenz et al. [22, 23] made use of this construct, implemented as $\mathbb{R} \times \mathbb{D}$, where $\mathbb{D}$ is the Poincaré disk model of the hyperbolic plane, for describing the effect of illumination changes in images. Besides that, hyperbolic geometry has not found much use within colour science.

In the current paper, the effect on colour metrics of using hyperbolic rather than Euclidean geometry for the chromatic plane is investigated. First, the transformation from Euclidean to hyperbolic geometry is described. Then, an experiment with well established Euclidean colour metrics and colour difference data sets is conducted and the results are compared to the state-of-the-art colour metric CIEDE2000.

2. Transformation to hyperbolic geometry

The Poincaré disk is one of the most commonly used models of the hyperbolic plane. It is defined as the open unit disk of the complex plane, $\mathbb{D} = \{z \in \mathbb{C} \mid |z| < 1\}$. Together with the metric or distance function on finite and infinitesimal form

$$d_{\mathbb{D}}(z_1, z_2) = 2\operatorname{artanh}\left|\frac{z_1 - z_2}{1 - z_1\bar{z}_2}\right|, \tag{1}$$

$$ds_{\mathbb{D}}^2 = \frac{4|dz|^2}{(1 - |z|^2)^2}, \tag{2}$$

this defines a two-dimensional plane of constant Gaussian curvature $K = -1$. For a thorough introduction to hyperbolic geometry and the Poincaré disk model, see, e.g., Anderson [24].

Consider a chromatic plane $\mathbb{R}^2$ with Cartesian coordinates (x, y) – representing, e.g., the a^* and b^* coordinates of CIELAB – with corresponding polar coordinates (r, θ), and an existing Euclidean metric. In using the Poincaré disk for modelling this chromatic plane, the radial distances should be kept unaltered under the transformation from Euclidean to hyperbolic geometry, since it is the hue super-importance, i.e., the increased angular distance, that we intend to model. This is obtained by the transformation

$$\tilde{r} = \tanh(r/2R), \tag{3}$$

if, at the same time, the Euclidean metric is exchanged with the scaled Poincaré disk metric,

$$d_R(\tilde{z}_1, \tilde{z}_2) = R d_{\mathbb{D}}(\tilde{z}_1, \tilde{z}_2), \tag{4}$$

were, $z_i = x_i + iy_i$, $\tilde{z}_i = \tilde{x}_i + i\tilde{y}_i$, $r_i = |z_i|$ and $\tilde{r}_i = |\tilde{z}_i|$. With this coordinate and metric transformation, we denote the resulting chromatic plane as $\mathbb{D}_R$, having a constant Gaussian curvature of $K = -1/R^2$.
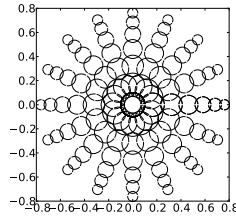
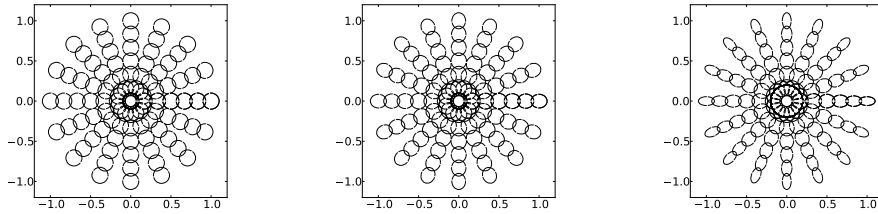Fig. 1. Equi-distant circles of radius r = 0.1 in the Poincaré disk model of hyperbolic geometry with $R = 1$.

Fig. 2. Equi-distant ellipses in the Euclidean plane according to the Poincaré disk metric d_r for various radii of curvature. Left to right: $R = \infty$ (Euclidean), $R = 1$, and $R = 0.5$.

In Euclidean geometry, curves of equi-distance to a point are equally sized circles, independent of the position in the plane. In the Poincaré disk model of hyperbolic geometry, the equi-distant curves are also circles, but with smaller radii as one moves towards the boundary, $\partial \mathbb{D}_R$, see Fig. 1. These circles can be transformed to ellipses in the Euclidean plane by using the inverse of the transform (3), and the method of Jacobians described in detail in Reference [10]. The corresponding equi-distant ellipses in the original chromatic plane are visualised in Fig. 2 for various values of R. It is instructive to study how the radius of curvature affects the ellipses. The higher the curvature, the more pronounced the elongation of the ellipses with increasing radial distance to the centre. This is exactly what is needed to model the hue super-importance effect. The geometry reduces to Euclidean geometry in the case when $R \to \infty$ (and thus $K \to 0$).

The metric can be extended to the three-dimensional case $\mathbb{R} \times \mathbb{D}_R$, where the lightness is represented along with the two chromatic coordinates, by means of the Euclidean product metric. In this way, the metric reduces to the Euclidean metric when $R \to \infty$ also in the three-dimensional case. In other words, if the original Euclidean coordinates are (L, x, y), the full metric is defined as

$$d((L_1, x_1, y_1), (L_2, x_2, y_2))^2 = (L_1 - L_2)^2 + (d_R(\tilde{z}_1, \tilde{z}_2))^2, \tag{5}$$

where $\tilde{z}_i$ are defined in terms of x_i and y_i as above.

3. Experiment

To test the hypothesis that a transformation from Euclidean to hyperbolic geometry will indeed improve the Euclidean colour metrics, a set of state-of-the-art Euclidean metrics are chosen and extended to hyperbolic geometry as described above. The best performing Euclidean metrics available today are the different versions of the DIN99 metric, i.e., DIN99, DIN99b, DIN99c, and DIN99d, as described by Cui [25], and the log-compressed OSA-UCS

metric ΔE_E by Oleari et al. [26]. As a baseline state-of-the-art non-Euclidean metric for comparison, the CIEDE2000 [9] is used.

The performance of these metrics is compared to existing data sets of colour pairs and colour discrimination ellipses and ellipsoids using standard statistical methods. The RIT-DuPont data set is an important available colour pair data set. It is provided as a set of T50-vectors of median values [27], and recently also as a full set of individual colour difference pairs [28]. For the full data set, also a set of weights inversely related to the uncertainty of the visual data is given. The performance of various metrics with respect to these data sets are commonly measured by the STRESS and WSTRESS methods, for the cases of unweighted and weighted data, respectively [29]. Thus, here we will use STRESS for the T50-values, and WSTRESS for the full data set. For the two measures, the statistical F-test can be used to evaluate the statistical significance of the performance of the metric. Since in our case we are looking for systematic variations of the metrics, it is meaningful to use also paired student's t-test. In addition to informing about the systematic improvements, paired tests are also normally stronger than unpaired ones. For each colour pair in the RIT-DuPont data sets, the metric is computed. Then, the output of the metric is scaled such that the average computed colour difference equals the average observed colour difference, ΔV, for both the original metric and the hyperbolically altered metric with the optimum choice of R (i.e., the minimum of the curves in Figs. 3 and 4, see below). Then, the squared error of the computed metrics with respect to ΔV can be compared with the paired t-test.

Adding to the paired data, we also test the resulting metrics against existing parametrised ellipse and ellipsoid data using the method by Farup and Pant [10], applying the paired statistical sign tests on the results as deviced by Pant et al. [30]. For this we use the BFD-P ellipses [31], and the three-observer data by Wyszecki and Fielder [32].

4. Results and discussion

Figures 3 and 4 show the STRESS and WSTRESS values for the prediction of the T50 and full RIT-DuPont data sets as a function of the radius of curvature, R, respectively, for the hyperbolic metrics derived from the selected Euclidean metrics. The dashed lines show the STRESS values for the corresponding Euclidean metric. The general trend is clear: The introduction of a negative curvature in the chromatic plane improves the metrics (i.e., reduces the STRESS and WSTRESS values) to a certain point where the curvature gets too large, and the STRESS and WSTRESS values increase rapidly. As $R \to \infty$, the STRESS and WSTRESS values approach the values for the corresponding Euclidean metrics, as expected. Although the trend is consistent, the lowest values of the curves are not statistically significantly lower than the corresponding values for the Euclidean metric according to the F-test commonly used for comparing STRESS and WSTRESS values [29].

Table 1 shows the p-values for two-sided paired t-tests for the full and T50 versions of the RIT-DuPont data set, as described above. For the the full data set, all the DIN99x metrics get a statistically significant improvement at the 1% confidence level by moving from Euclidean to hyperbolic geometry. Three of the DIN99x metrics get significant improvenents also at the 5% confidence level for the reduced T50 data set. For the ΔE_E metric, the improvement by the transition from Euclidean to hyperbolic geometry is not statistically significant.

The fitting of the ellipsoids to the BFD-P ellipses [31], and the three-observer data by Wyszecki and Fielder [32] was compared using the method described in detail in References [10, 30], and analysed with the statistical sign test. For both of these data sets, the improvement of the metrics by going from Euclidean to the hyperbolic version with the radius of curvature optimised on the T50 data set is statistical significant at the 1% level for all of the Euclidean metrics included in this study.
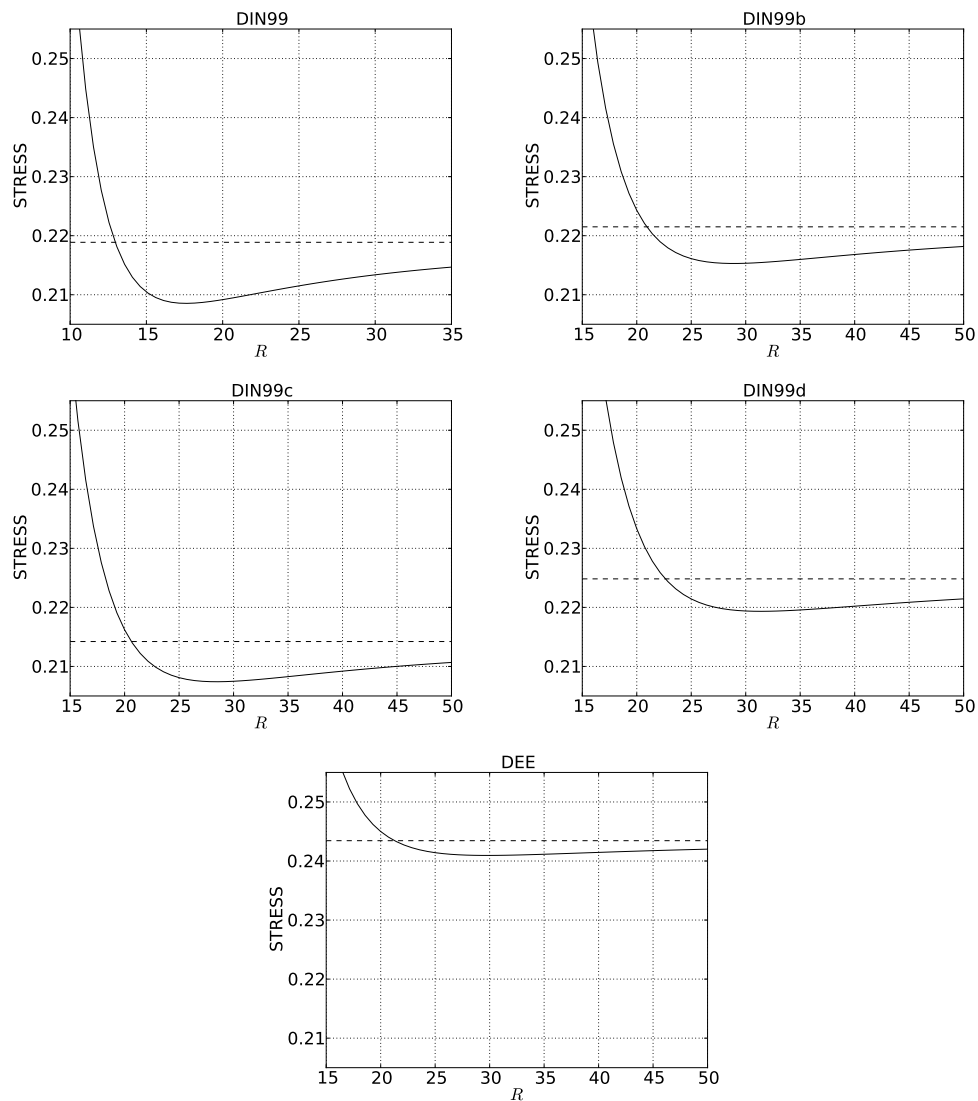
Fig. 3. STRESS values for the prediction of the RIT-DuPont T50 data set for the hyperbolic metrics derived from the given Euclidean metrics as a function of the radius of curvature, R. The dashed lines show the STRESS values for the corresponding Euclidean metric.
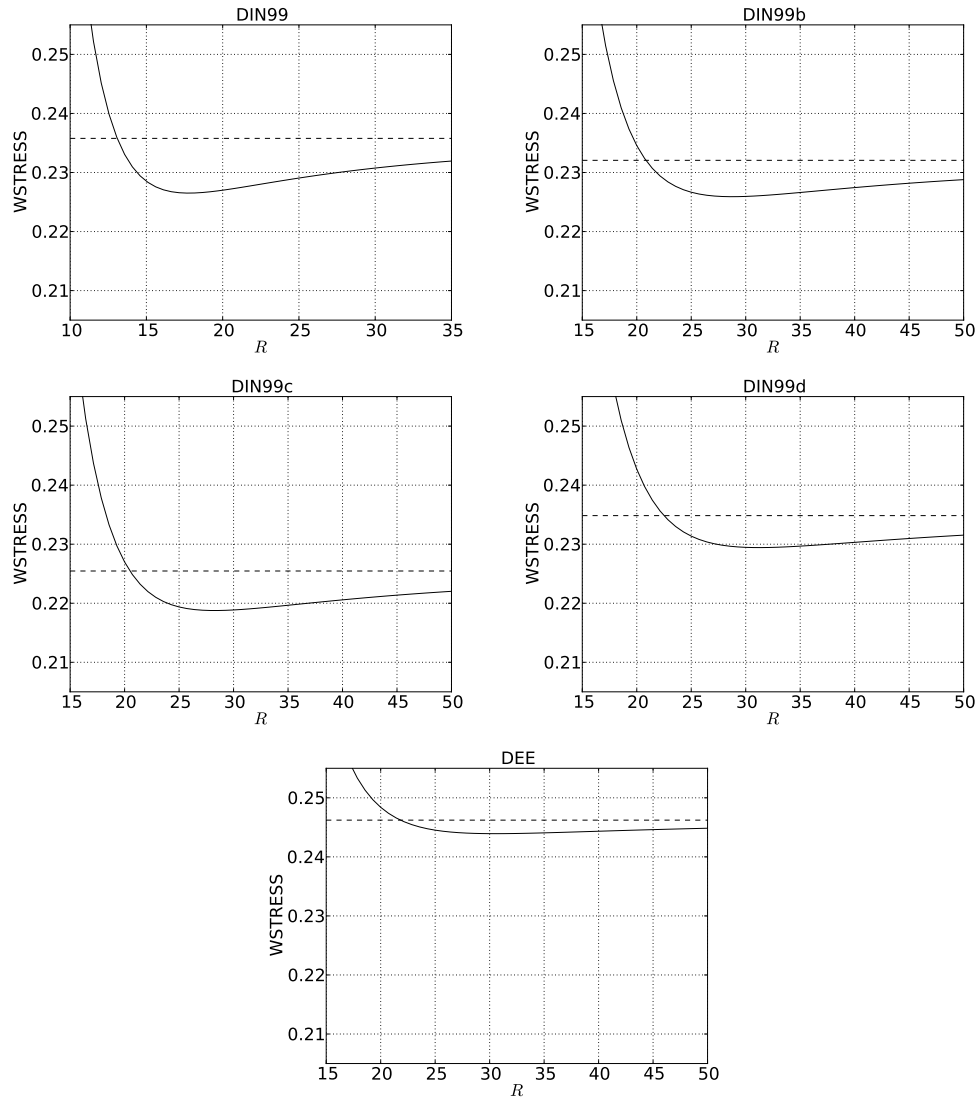
Fig. 4. WSTRESS values for the prediction of the full RIT-DuPont data set for the hyperbolic metrics derived from the given Euclidean metrics as a function of the radius of curvature, R. The dashed lines show the WSTRESS values for the corresponding Euclidean metric.

Table 1. *p*-values for two-sided paired *t*-tests for the full and T50 versions of the RIT-DuPont data set for the difference between the standard Euclidean and the suggested hyperbolic improvement of the metric.

Metric	T50	Full
DIN99	0.0014	$7.6 \cdot 10^{-5}$
DIN99b	0.034	0.0021
DIN99c	0.017	0.0012
DIN99d	0.058	0.0066
ΔE_E	0.23	0.095

It is well established in the literature – and confirmed by the computations here – that none of these Euclidean metrics perform significantly better than DE2000. Table 2 shows the *p*-values for a two-sided paired *t*-test for the full and T50 versions of the RIT-DuPont data set for the difference between the suggested hyperbolic improvement of the Euclidean metrics versus DE2000. The table shows that for most of the metrics, the differences are not statistically significant. However, the hyperbolic version of DIN99c – the already best performing DIN99x metric on these data sets – performs statistically significantly better than the DE2000 metric at the 5% significance level for both data sets.

Table 2. *p*-values for two-sided paired *t*-tests for the full and T50 versions of the RIT-DuPont data set for the difference between the suggested hyperbolic improvement of the metric and DE2000.

Metric	T50	Full
DIN99	0.17	0.092
DIN99b	0.092	0.061
DIN99c	0.039	0.026
DIN99d	0.26	0.49
ΔE_E	0.25	0.13

Figure 5 shows the cross-sections of the equi-distant ellipsoids for the RIT-DuPont data set as fitted by Melgosa [33] together with the corresponding plain DIN99 ellisoids and the version of DIN99 in the hyperbolic colour space. The improvement in the fit of the ellipsoids is small, but clearly noticable.

The circumference of a circle in hyperbolic geometry is $2\pi R \sinh(r/R) > 2\pi r$. The optimal radius of curvature for the DIN99c hyperbolic space with respect to the RIT-DuPont data is $R = 28.6$. For comparison, the most saturated Munsell renotation colour [1] has a chroma of 60.6 in the DIN99c space. The ratio of the circumference of the hyperbolic circle with radius 60.6 to the Euclidean circle of the same radius is 1.94, i.e., close to 2. According to Judd [2], the circumference of the hue circle for saturated colours should be $4\pi r$, rather than $2\pi r$ due to the hue super-importance effect. This corresponds very well with the observed radius of curvature found here from optimising the local colour metric.

It could be argued that introducing a new parameter necessarily must lead to an improvement of the fit with the observational data. However, the fact that all the metrics are consistently improved with a finite choice of R is a strong indication that the chromatic plane is indeed negatively curved. If, on the other hand, the chromatic plane were positively curved, a mapping to hyperbolic geometry could only make things worse, and the optimisation would cause $R \to \infty$, and the best fit would in other words be the the Euclidan space.

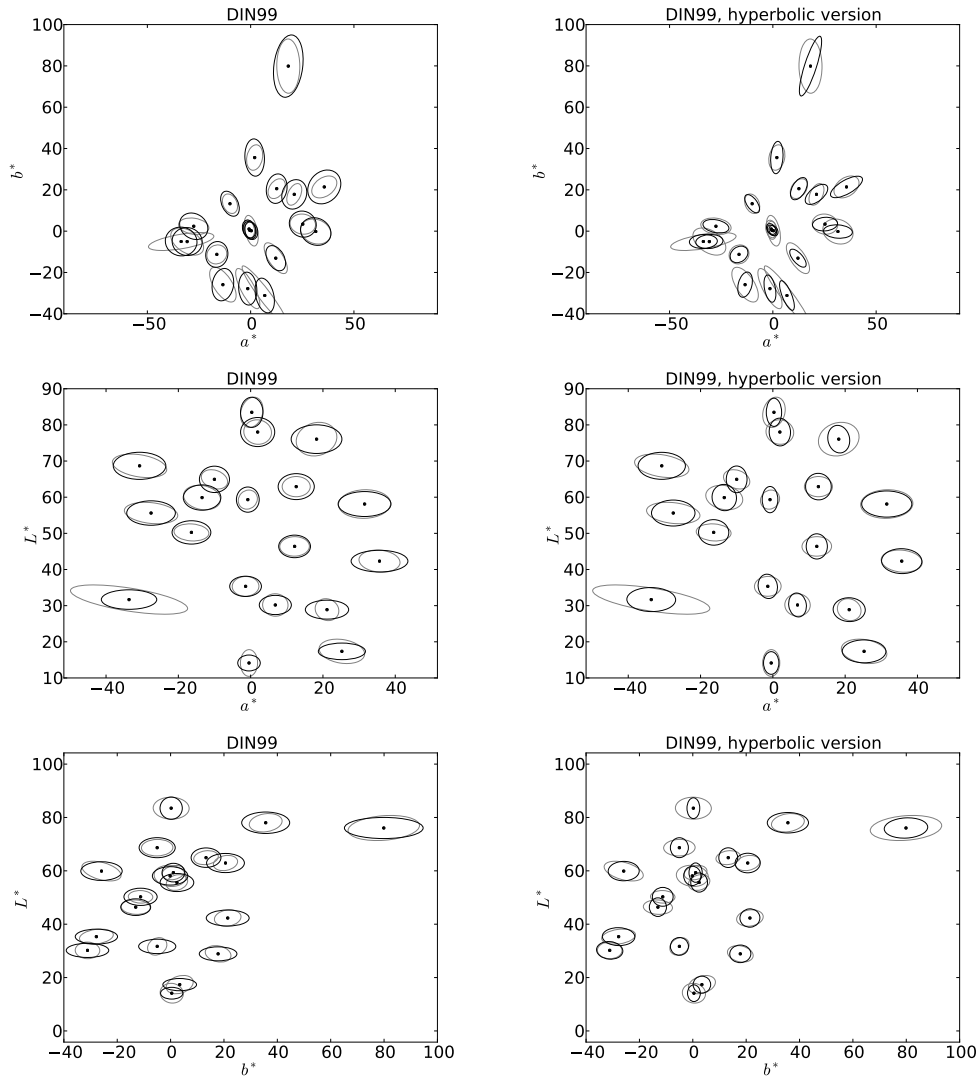The underlying colour spaces of all the Euclidean colour metrics tested here have been op-

Fig. 5. Various cross sections in the CIELAB space of Melgosa's fitted ellipsoids for the RIT-DuPont data set (grey) and computed ellipsiod cross sections (black) for the standard DIN99 metric (left) and the hyperbolic version of the DIN99 metric (right).

timised for giving best results with Euclidean metrics. It is therefore reasonable to assume that if the underlying colour space were optimised for the hyperbolic metric, even better results could be achieved. It is also worth noting that all the metrics perform better on the T50 data set than on the full RIT-DuPont data set. One possible explanation for this is that the underlying metrics have been optimised for the reduced data set. It should also be noted that the colour metric observational data is noisy, observer dependent, and time dependent, and that the databases used are relatively small. Thus, the detailed parameter values obtained in optimisations such as the current one, should not be taken too literally. With this as a background it is even more fascinating that the optimisations on the local noisy data still give relatively consistent results for the magnitude of the negative curvature of the chromatic plane, and that this curvature corresponds well with the globally observed hue super-importance phenomenon.

5. Conclusion

It is demonstrated that state-of-the-art Euclidean colour metrics can be statistically significantly improved by moving from Euclidean to hyperbolic geometry for the representation of the chromatic plane. It is also shown that one of the hyperbolic metrics derived from the existing Euclidean one can outperform even the state-of-the-art non-Euclidean metric CIEDE2000. Hyperbolic geometry also nicely models the hue super-importance effect observed in colour order systems. When the radius of curvature of the hyperbolic chromatic plane is optimised to give as good fit with colour metric data as possible, the magnitude of the resulting hue super-importance effect is on the order of what has been previously estimated for the purpose of colour order systems. This suggests that negatively curved colour spaces should be taken into consideration in the future development of colour metrics and colour spaces.